Electronic Supplementary Material (ESI) for RSC Advances.

Supplementary Figures

Figure S1

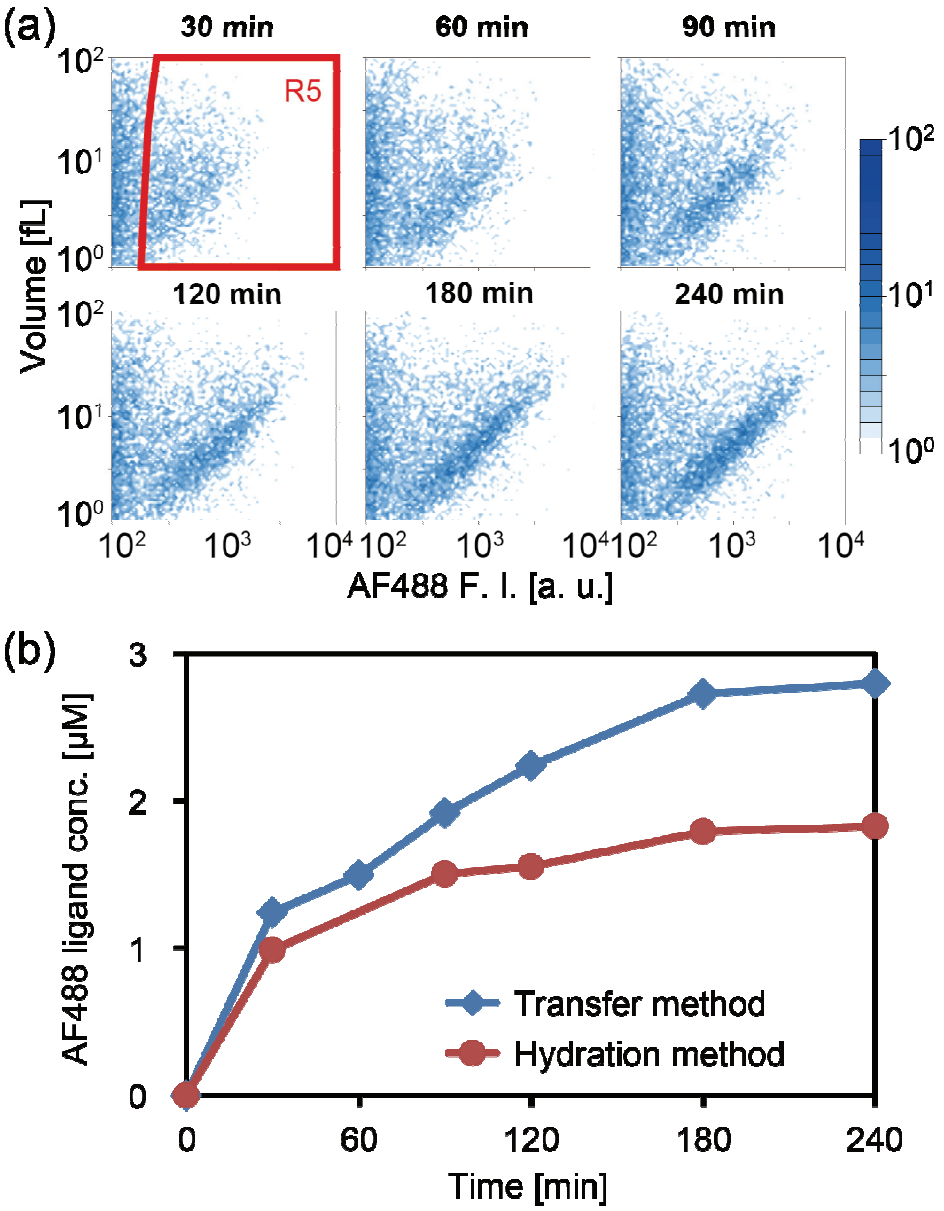

Figure S1. The time course of accumulation of fluorescence in AF488 ligand-permeable vesicles. (a) 2D plot of the vesicle size and fluorescence intensity for the AF488 ligand obtained by FCM. Only a fraction of the vesicles showed an increase in fluorescence intensity over time. The data were acquired using GUVs prepared by the transfer method. (b) The time course of changes in

AF488 ligand concentration inside the AF488 ligand-permeable vesicles prepared by the transfer (blue) and hydration (red) methods. The data represent the average AF488 concentration at each time point and are estimated from the FCM data shown in (a). All vesicles in gate R5 were used to estimate the concentration of the AF488 ligand. Each ligand concentration was calculated from the analytical curve indicating the relationship between ligand concentration and fluorescence level. To make the analytical curve, 5 μM HaloTag protein was labeled with different concentrations of AF488 ligand, the labeled HaloTag protein was encapsulated in GUVs individually, and the green fluorescence intensity was measured by FCM.

Permeability coefficients for the AF488 ligand and the TMR ligand were estimated from these data, as described below. According to Fick's law, the amount of a solute (N_{ligand}) that has penetrated through a membrane area A at time t can be written as follows:

$$\begin{aligned} J &= D\frac{\beta}{l}\Delta C_{\mathrm{ligand}} \\ &= P\Delta C_{\mathrm{ligand}} \\ &= \frac{N_{\mathrm{ligand}}}{At} \end{aligned} \qquad \textbf{Eq. S1}$$

in which J is the flux, D is the diffusion constant, β is the distribution coefficient, l is the membrane thickness, P is the permeability coefficient, and $\Delta C_{\mathrm{ligand}}$ is the difference in concentration of the solute across the membrane. When considering the permeation events that occur from the exterior to the interior of a single vesicle with a volume V, N_{ligand} at time t can also be written as follows:

$$N_{\mathrm{ligand}} = C_{\mathrm{ligand}} V \qquad \textbf{Eq. S2}$$

in which C_{ligand} is the solute concentration inside the vesicle. From *Eqs. S1* and *S2*,

$$P\Delta C_{\text{ligand}} = \frac{C_{\text{ligand}} V}{At} \qquad \textbf{Eq. S3}$$

If the diameter of the vesicle is assumed to be d, the above equation can be written as follows:

$$P = \frac{C_{\text{ligand}}\, d}{6\Delta C_{\text{ligand}}\, t} \qquad \textbf{Eq. S4}$$

For the AF488 ligand, we used t = 1800 s and C_{ligand} = 1.2 μM and 1.0 μM for the transfer and hydration methods, respectively. As we added 20 nM AF488 ligand to the outside of the vesicle, we assumed that ΔC_{ligand} = 20 nM. While the vesicle size has some variability, we estimated the P value for an average-sized vesicle, i.e., d = 3 μm. From these values, we obtained $P = 1.7\times10^{-6}$ and 1.4×10^{-6} cm/s for the transfer and hydration methods, respectively.

For the TMR ligand, we used t = 300 s and C_{ligand} = 30 μM. As we added 1 μM TMR ligand to the outside of the vesicle, we assumed that ΔC_{ligand} = 1 μM. While the vesicle size had some variability, we estimated the P value for an average-sized vesicle, i.e., d = 3 μm. From this value, we obtained $P = 5\times10^{-6}$ cm/s.

Figure S2

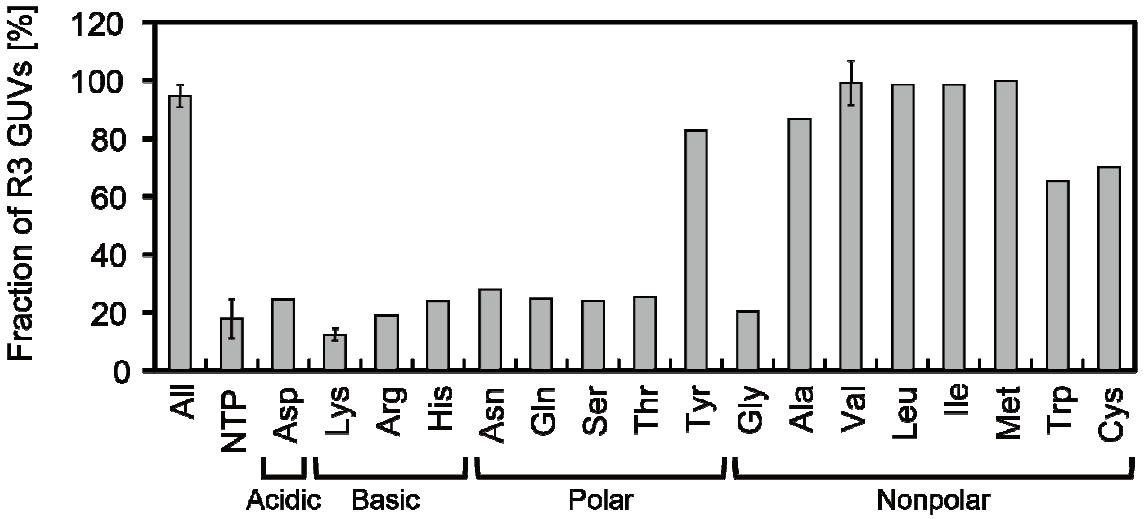

Figure S2. The membrane permeabilities of various low molecular weight components contained in the PURE system were investigated. The horizontal axis shows the names of low molecular weight components used. "All" indicates conditions in which all of the components were encapsulated in GUVs. This result shows that GFP synthesis was possible in almost all GUVs. The vertical axis indicates the proportion of GUVs contained in the R3 region, as shown in Figure2 (b). GUVs produced by the transfer method were used in all of the experiments.

Figure S3

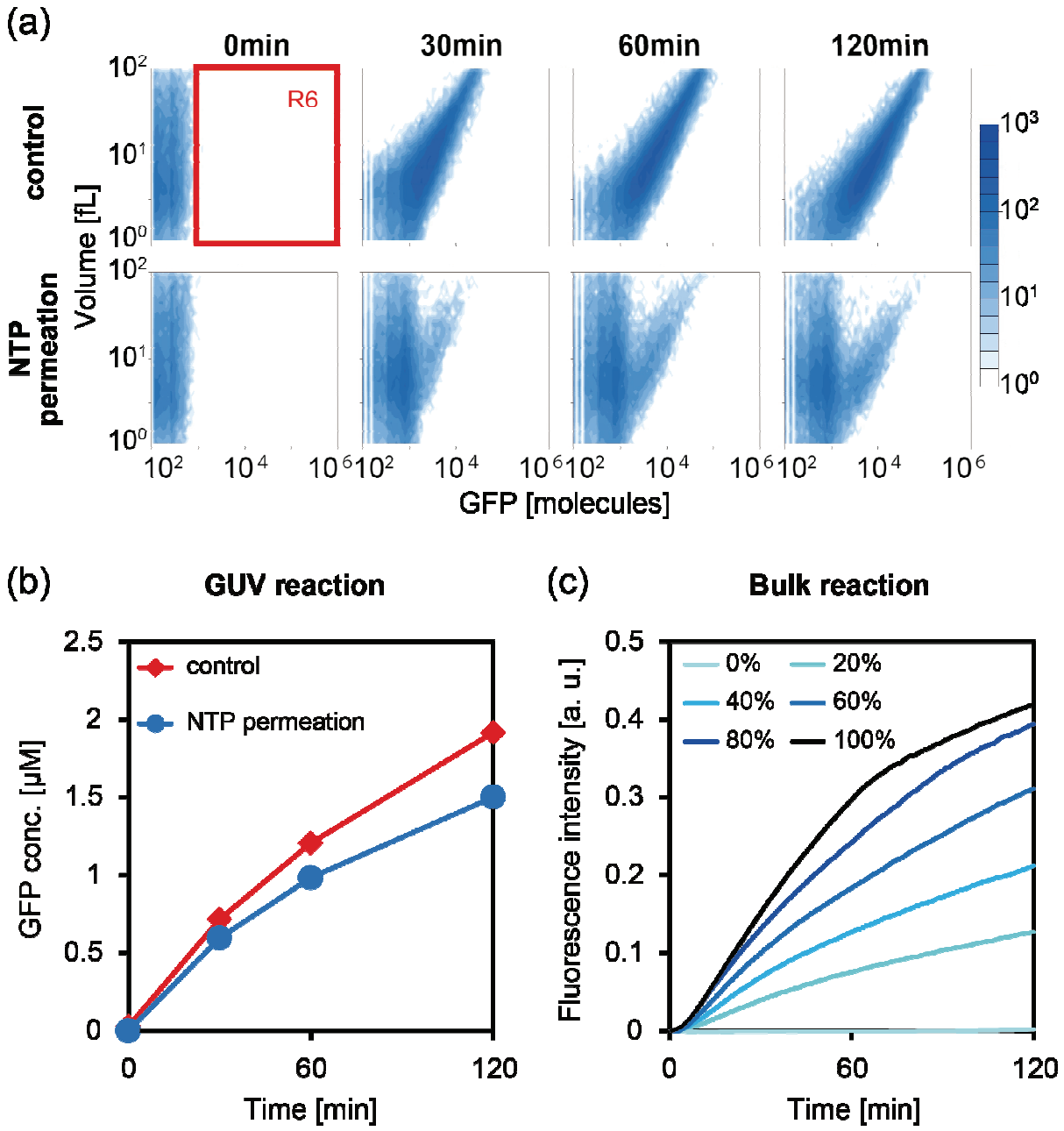

Figure S3. The time course of GFP synthesis in NTP-permeable vesicles. (a) 2D plot of the vesicle size and the number of GFP molecules per vesicle obtained by FCM. When the GUVs containing all components of the PURE system were prepared, GFP synthesis occurred in the entire population (control). However, when GUVs lacking NTPs were prepared and NTPs were

supplied to the exterior of the vesicles, GFP was only synthesized in a fraction of the vesicles (NTP permeation). (b) The time course of GFP synthesis inside the GUVs. The data shown are the average GFP concentration at each time point and were estimated from the FCM data shown in (a). All vesicles in gate R6 were used to estimate the GFP concentrations in the "control" and "NTP permeation" data. (c) GFP synthesis using the PURE system in a batch reaction with different NTP concentrations. A value of 100% indicates that the concentration of NTPs used was the default concentration given in Table S1. GUVs produced by the transfer method were used in all of the experiments.

The permeability coefficient for the NTPs was estimated from these data as described below. From Eq. S5, we obtain

$$P = \frac{C_{\mathrm{NTPs}} d}{6 \Delta C_{\mathrm{NTPs}} t} \qquad \textbf{Eq. S5}$$

in which C_{NTPs} and ΔC_{NTPs} are the concentrations of NTPs inside the vesicle and the difference in NTP concentration across the membrane, respectively. From the experimental data, at t = 1800 s, C_{NTPs} was estimated to be 60% of the outer solution (i.e., A:G:C:U = 2.25:1.5:0.75:0.75 mM). We estimated the P value for an average-sized vesicle, i.e., d = 3 μm. From these values, we obtained $P = 1.7 \times 10^{-8}$ cm/s.

Figure S4

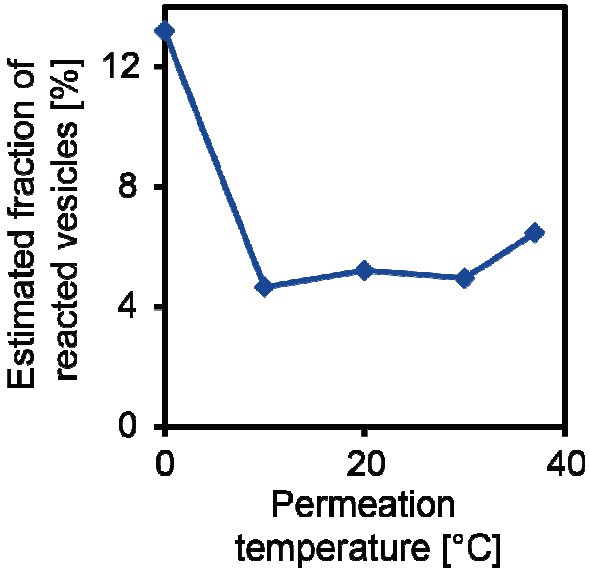

Figure S4. Effects of incubation temperature on the fraction of NTP-permeable vesicles. The GUVs used to evaluate the permeability of the NTPs were prepared as described in the main text. After preparing the GUVs at 4°C, the NTPs were added to the vesicle suspension at different temperatures (between 0°C and 37°C), and the GUVs were incubated at this temperature for 10 min. The vesicles were then warmed to 37°C and incubated for a further 4 h to perform GFP synthesis. The fraction of reacted vesicles was estimated by FCM, as shown in Figure 2. GUVs produced by the transfer method were used in all of the experiments.

Figure S5

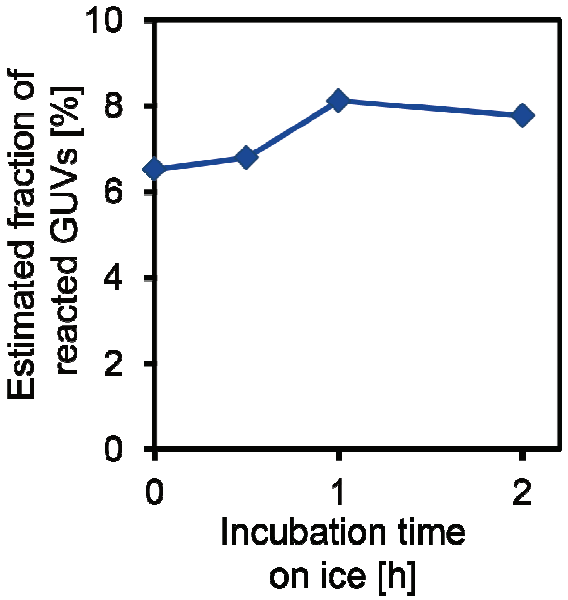

Figure S5. Effects of the incubation time on ice on the fraction of NTP-permeable vesicles. The GUVs used to evaluate the permeability of NTPs were prepared as described in the main text. After preparing GUVs at 4°C, the vesicles were incubated on ice for varying amounts of time (between 0 and 2 h) prior to adding the NTPs at 37°C. The vesicles were then warmed to 37°C and incubated for a further 4 h to perform GFP synthesis. The fraction of reacted vesicles was estimated by FCM, as shown in Figure 2. GUVs produced by the transfer method were used in all of the experiments.

Figure S6

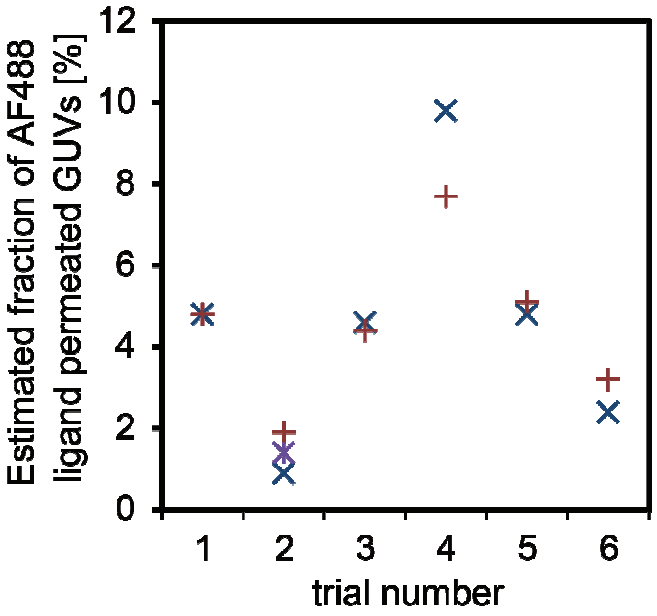

Figure S6. Batch-to-batch variation in the fraction of permeable GUVs. The horizontal axis shows the trial number, and the vertical axis shows the estimated fraction of AF488 ligand-permeable vesicles, as shown in Figure 1. The GUVs were prepared using the transfer method with POPC. For each trial, two or three batches of GUVs were prepared that showed very similar permeabilities (CV approximately 13%), whereas the average value among the trials showed much larger variation (CV approximately 55%).

Supplementary Text

Estimation of membrane-defect area, expediently regarded as sum of the pore size. According to Fick's law, the amount of solute permeating through n pores of A_{pore} in area during time t (N_{ligand}) is indicated by the following formula:

$$J_{pore} = \frac{N_{\text{ligand}}}{nA_{pore}t} \qquad \text{Eq. S6}$$

in which J_{pore} is the flux. Using the Stokes–Einstein equation, J_{pore} can be written as follows:

$$J_{pore} = D\frac{\beta}{l}\Delta C = \frac{k_B T}{6\pi\eta r}\frac{\beta}{l}\Delta C \qquad \text{Eq. S7}$$

in which D is the diffusion constant, β is the distribution coefficient, l is the membrane thickness, ΔC is the difference in solute concentration across the membrane, η is the viscosity of the solute, r is the radius of the HaloTag ligand, k_{B} is the Boltzmann constant, and T is the temperature.

J_{pore} was estimated for the HaloTag ligand in 1 M sucrose by substituting the values described as follows. The term β was defined as 1 because we assumed the presence of a pore. The term l was defined as 5×10^{-9} m [1], η was defined as 3×10^{-4} kg/m·s, which is a typical value for a 1 M sucrose solution [2], and r was defined as 0.25 nm, which is a typical size for a molecule of this molecular weight. As we added 20 nM HaloTag ligand to the outside of the vesicle, we assumed that ΔC = 20 nM.

When considering the permeation events occurring from the exterior to the interior of a single vesicle with a volume of V, N_{ligand} at time t can also be written as shown in Eq. S2 (Figure S1). The sum of membrane-defect area, regarded as one (n=1) or more (n>1) pores (nA_{pore}) obtained by formulas S2, S6, and S7 was 2 nm^2.

Supplementary Tables

Table S1. Composition of the components included in the PURE system. All protein components were prepared as described previously [3]. *D-Glutamic acid was used as the salt because we found trace quantities of amino acids other than glutamic acid in the L-glutamic acid potassium salt, which interfered with the permeability measurements for each amino acid, as shown in Figures 2 and S2.

Name	**Concentration**
Initiation factor 1	24700 nM
Initiation factor 2	1030 nM
Initiation factor 3	1210 nM
Elongation factor G	1080 nM
Elongation factor Tu	80200 nM
Elongation factor Ts	3300 nM
Release factor 1	49 nM
Release factor 2	48 nM
Release factor 3	168 nM
Ribosome recycling factor	3880 nM
Alanyl-tRNA synthetase	727 nM
Arginyl-tRNA synthetase	31 nM
Asparaginyl-tRNA synthetase	420 nM
Aspartyl-tRNA synthetase	121 nM
Cysteinyl-tRNA synthetase	24 nM
Glutaminyl-tRNA synthetase	60 nM

Glutamyl-tRNA synthetase	232 nM
Glycyl-tRNA synthetase	86 nM
Histidyl-tRNA synthetase	85 nM
Isoleucyl-tRNA synthetase	365 nM
Leucyl-tRNA synthetase	41 nM
Lysyl-tRNA synthetase	115 nM
Methionyl-tRNA synthetase	109 nM
Phenylalanyl-tRNA synthetase	134 nM
Prolyl-tRNA synthetase	166 nM
Seryl-tRNA synthetase	78 nM
Threonyl-tRNA synthetase	84 nM
Tryptophanyl-tRNA synthetase	28 nM
Tyrosyl-tRNA synthetase	152 nM
Valyl-tRNA synthetase	17 nM
Methionyl-tRNA formyltransferase	588 nM
Myokinase	1340 nM
Creatine kinase	248 nM
Nucleoside-diphosphate kinase	16 nM
Pyrophosphatase	41 nM
Tig	1000 nM
HrpA	100 nM
Ribosome	3000 nM
20 amino acid mix	0.3 mM
ATP	3.75 mM
GTP	2.5 mM
CTP	1.25 mM

UTP	1.25 mM
Transfer RNA mix	24 μg/μL
HEPES–KOH, pH 7.6	100 mM
10-formyl-5,6,7,8-tetrahydrofolic acid	0.01 μg/μL
Glutamic acid, potassium salt	280 mM
Spermidine	1.5 mM
Magnesium acetate	20 mM
Creatine phosphate	25 mM
Dithiothreitol	1.5 mM

References

1. Boal, D. H., *Mechanics of the cell*. Cambridge University Press: Cambridge, UK ; New York, 2002; p xiv, 406 p.

2. Nagasawa, Y.; Nakagawa, Y.; Kenmochi, J.; Okada, T., Microscopic viscosity of aqueous solution of saccharides: A study by ultrafast pump-probe spectroscopy. *Cryobio. Cryotech* **2003,** 49, 87-95.

3. Matsuura, T.; Kazuta, Y.; Aita, T.; Adachi, J.; Yomo, T., Quantifying epistatic interactions among the components constituting the protein translation system. *Mol Syst Biol* **2009,** 5, 297.